EurJIC European Journal of Inorganic Chemistry
ChemPubSoc Europe
FULL PAPER

DOI:10.1002/ejic.201301612

On the Investigation of the Droplet–Droplet Interactions of Sodium 1,4-Bis(2-ethylhexyl) Sulfosuccinate Reverse Micelles upon Changing the External Solvent Composition and Their Impact on Gold Nanoparticle Synthesis

Jorge A. Gutierrez,[a] R. Dario Falcone,[a] M. Arturo Lopez-Quintela,[b] David Buceta,[b] Juana J. Silber,[a] and N. Mariano Correa*[a]

Keywords: Organized systems / Nanoparticles / Interfaces / Surfactants / Reverse micelles / Solvent effects

The effect of the composition of the nonpolar organic media on the properties of sodium 1,4-bis(2-ethylhexyl) sulfosuccinate (AOT) reverse micelles (RMs) at a fixed temperature were investigated. To monitor interfacial micropolarity and sequestrated water structure in *n*-heptane:benzene/AOT/water RMs, the solvatochromic behavior of coumarin 343 (C343) as an absorption and emission probe was studied, and the size of the droplets was measured by dynamic light scattering (DLS). The DLS results confirm the formation of the *n*-heptane:benzene/AOT/water RMs at every *n*-heptane mole fraction investigated. The data show that as the *n*-heptane content increases, the interdroplet attractive interactions and the droplet size both increase. With C343 spectroscopy, we determined the "operational" critical micellar concentration, the interfacial micropolarity of the RMs, the hydrogen-bond ability of the media, and the sequestrated water structure in every RM system studied. To verify the modulation of the interdroplet interactions by the external solvent, we have used a well-known synthetic method to create gold nanoparticles in different RM media. The results support the conclusion that the droplet–droplet interactions are favored with *n*-heptane as the nonpolar solvent. Thus, the rate of material exchange among micelles increases, and small, monodispersed, and highly concentrated gold nanoparticles are formed. The situation is different for AOT RMs prepared in benzene, in which subnanometer gold clusters are produced. The formation of clusters instead of nanoparticles reflects poor material exchange among the micelles owing to unfavorable droplet–droplet interactions. In this way, our results offer a new appealing way to focus the production of nanoparticles into subnanometer clusters, which is one of the hottest current topics in nanoparticle synthesis. Therefore, it is possible to dramatically affect different properties of the RMs by changing the solvent blend; such effects cannot be obtained with only a single solvent composition and may have a large impact on nanotechnology. We anticipate remarkable effects on nanoparticle sizes and polydispersity with different organic solvent blends.

Introduction

Reverse micelles (RMs) are of considerable practical importance in different areas such as detergents, foodstuffs, and cosmetics.[1,2] RMs are supramolecular assemblies formed when surfactants are dissolved in nonpolar organic solvents. Their polar area is located in the interior (core), and their hydrocarbon tails extend into the organic nonpolar solvent.[1,3,4] Different anionic, cationic, and nonionic surfactants have been employed to prepare RMs in nonpolar solvents.[1–12] Among the anionic surfactants that form RMs, the best known are the systems made with so-

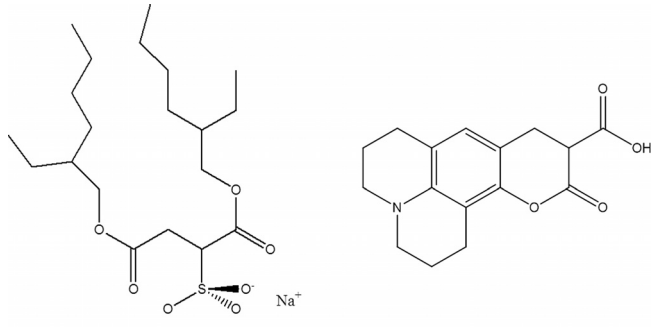

Scheme 1. Molecular structures of the surfactant AOT and molecular probe C343.

[a] Departamento de Química, Universidad Nacional de Río Cuarto,
Agencia Postal # 3, C. P. X5804BYA Río Cuarto, Argentina
E-mail: mcorrea@exa.unrc.edu.ar
http://gso-unrc.blogspot.com.ar/
www.unrc.edu.ar
[b] Facultad de Química, Departamento de Química-Física, Laboratorio de Nanotecnología y Magnetismo (NANOMAG), Universidad de Santiago de Compostela,
C. P. 15782 Santiago de Compostela, Spain
Supporting information for this article is available on the WWW under http://dx.doi.org/10.1002/ejic.201301612.

dium 1,4-bis(2-ethylhexyl) sulfosuccinate (AOT; Scheme 1) in different solvents. AOT forms spherical RMs in aromatic and hydrocarbon solvents without the addition of a cosurfactant, and water can be solubilized up to W_0 = [H_2O]/[surfactant] ≈ 60, depending on the external solvent and temperature.[1,3,4]

RMs are thermodynamically stable systems over wide composition and temperature ranges,[1,3,4,13] and it is generally supposed that AOT RMs behave like hard spheres with a small attractive potential that depends on different parameters such as temperature, W_0, the presence of electrolyte, and the external solvent.[9,13] Different physical phenomena are observed in these systems, such as electrical conductivity percolation and phase transition,[13] all of which have the same origin: the droplet–droplet interaction. It is not necessary to achieve the phase transition of the system to observe the effects of the droplet–droplet interactions. For example, at a fixed temperature within the reverse micellar stability region of the phase diagram, the interaction is manifested by an increase of the droplet size.[1,9,14–16] Changing the composition of the RMs also changes the droplet size and the interdroplet interaction,[17] and the attraction between droplets also depends on the fluidity of the interface.[17,18] Lemaire et al. proposed that the attractive droplet–droplet interactions depend on the mutual interpenetration of the surfactant tails over some small distance without much entropy loss and a decrease in the total free energy of the system.[19] This is possible because the surfactant tail–tail interactions are not much stronger than the surfactant–nonpolar-external-solvent interactions. At a fixed temperature, the solvent molecules are not optimally oriented to interact with the surfactant tails, whereas the surfactant tails of two different RMs in the overlap region are always more or less parallel to each other.[19,20] The overlap between micelles is accompanied by the removal of nonpolar organic solvent,[19] and Calje et al. also proposed that these interactions are the result of differences in the molecular composition between the droplets and the external organic solvent.[21]

With regard to the external nonpolar solvent, the phase behavior and/or the properties of microemulsions can be affected by changes to the composition of the nonpolar solvent.[14–16,22,23] Thus, it is possible to control the stability of RMs by applying mixtures of different solvents to create the aggregates. The solvents can be denominated as "good" and "bad" solvents, depending on whether they decrease or increase the attractive droplet–droplet interactions, respectively. Thus, it is possible to induce aggregations (flocculation) of RMs by using solvent blends, and this results in a method that is economical and of potentially low energy consumption. This approach could be applied in separation technology to nanoparticulated systems of high value to redisperse and reuse the active components without affecting the functionality of the RMs.[14–16]

Although the properties of RMs depend on the type of surfactant, the W_0 values,[1–4,24,25] and the external nonpolar organic pseudophase, little research has been performed on the influence of the organic media for AOT,[10,26–31] and this influence has only been investigated very recently for the cationic RMs formed with the benzyl-*n*-hexadecyldimethylammonium chloride (BHDC) surfactant.[22,23] On the other hand, although droplet–droplet interactions play a predominant role in the size control of RMs, it is also necessary to understand the nature of the RM interfaces because mass transfer is not possible unless the interface is disrupted.[26] To the best of our knowledge, there are no studies of AOT RMs that use a molecular probe to investigate the effect of the external nonpolar solvent on the interfacial properties within the reverse micellar phase of the phase diagram, which is far from the percolation of the system. We believe that with this contribution we can make a step towards a full understanding of the interfacial properties of AOT RMs; such an understanding is mandatory to take control of the separation technology of high-value nanoparticle synthesis, for example.

Coumarin 343 (C343, Scheme 1) was chosen as the molecular probe as it has been fully characterized as a probe in different laboratories, including ours (see Supporting Information).

In this work, *n*-heptane:benzene/AOT/water RMs were investigated by dynamic light scattering (DLS) and the solvatochromism of C343 at a fixed temperature. To evaluate interesting RM interfacial properties, we studied the surfactant, the water dissolved, and the external organic solvent content. DLS experiments showed that AOT RMs formed in every *n*-heptane:benzene blend investigated and, at a given W_0 value, the droplet size increased as the *n*-heptane content increased. Under this scenario, C343, a molecular probe that resides at the RM interface, shows a less polar environment in which its intramolecular hydrogen-bond interactions prevail and it favors the monomer species (see Supporting Information). We have discussed the results and considered how the solvent penetration into the interface affects the droplet–droplet interaction. To verify the modulation of the interdroplet interactions owing to the external solvent, we have used a well-known gold nanoparticle synthesis[32,33] in two different RM systems, namely, benzene/AOT and *n*-heptane/AOT, both of which are extreme cases. A wide range of techniques for the synthesis of metal nanoparticles have been developed in recent years to control their size and shape; among these techniques is the use of RMs.[32,33] Moreover, as the nanoparticle synthesis is based on Brownian motion and on interactions between droplets that form fused dimers (or encounter pairs) in which the reactants are exchanged, we hypothesize that by changing the external solvent composition, different nanoparticle sizes may be obtained. In these systems, nanoparticles are formed in chemical reactions controlled by intermicellar exchange of the reagent molecules and ions initially present in different micelles. Despite its relative simplicity and accessibility, this technique affords the preparation of monodispersed nanoparticles with a tunable size,[34] as many properties, not only physical but also biological and chemical, strongly depend on these parameters (monodispersity and size).[35,36] We want to emphasize that our goal is to go beyond the gold nanoparticle formation processes by delv-

ing into the complex mechanisms involved in the nanoparticle synthesis in RMs and highlighting the importance of the solvent composition on the interdroplet interactions. Moreover, the results shown here can offer a simple way to direct the nanoparticle synthesis in RMs into subnanometer clusters, an area of especial interest because of their very important catalytic applications.[37,38]

Results and Discussion

Studies in *n*-Heptane:Benzene/AOT Reversed Micelles

The first experiment performed was to evaluate the maximum amount of water (W_{0Max}) that the AOT RM systems can accept to give a transparent and stable single phase as a function of the *n*-heptane mole fraction X_{Hp} (Table 1). Interestingly, AOT is a surfactant that can form RMs in pure benzene and *n*-heptane with W_{0Max} = 12 and 60, respectively.[3]

Table 1. Maximum W_0 (W_{0Max}) values obtained in AOT RMs at different *n*-heptane mole fractions (X_{Hp}). [AOT] = 0.1 M.

X_{Hp}	W_{0Max}
0.00	12
0.06	12
0.37	18
0.84	55
1.00	60

From Table 1, it is clear that the W_{0Max} values increase as the *n*-heptane content increases, as is expected. Nevertheless, a question may arise here about why water can be solubilized in larger amounts as the polarity of the organic pseudophase decreases. We consider that the key to answer this question is in the composition of the AOT RM interface, that is, how the effective interfacial composition is modified as the solvent blend changes. To the best of our knowledge, there have been no systematic studies at the molecular level in which the AOT interfacial composition was monitored. To know this, it is necessary to gain insights into mass transfer processes between droplets, a mandatory step in the nanoparticle synthesis in reverse micelles.

DLS was used to assess whether the water is effectively encapsulated by the surfactant to create a true RM in the AOT/water in the different *n*-heptane:benzene blends investigated, as described previously.[3,4,39–42] Thus, if water is really encapsulated to form RMs, the droplet size must increase linearly as the W_0 value increases (swelling law of RMs), as is well established for water or polar solvent/surfactant RM systems.[3,39] This feature can also demonstrate that the *n*-heptane:benzene/AOT/water RMs consist of discrete more or less spherical droplets.[40]

In Figure 1 and Table 2, we report the apparent hydrodynamic diameter (d_{App}) values obtained in *n*-heptane:benzene/AOT/water systems at different X_{Hp} values. As can be seen in all the systems studied, there is an increase in the d_{App} values when the W_0 value increases.

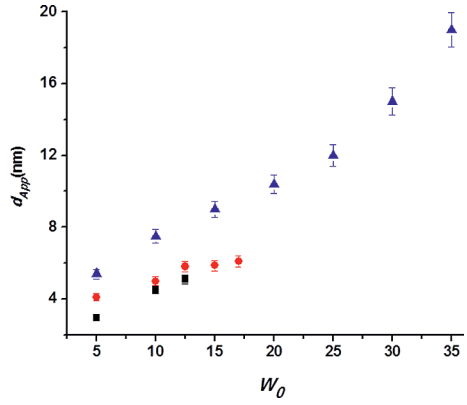

Figure 1. Apparent hydrodynamic diameter (d_{App}) of the droplets for *n*-heptane:benzene/AOT/water as a function of W_0. [AOT] = 0.1 M, X_{Hp} = 0.0 (black squares), 0.37 (red circles), and 1.0 (blue triangles).

Table 2. Apparent hydrodynamic diameter (d_{App}) of AOT reverse micelles with increasing W_0 parameter at different *n*-heptane mole fractions (X_{Hp}). [AOT] = 0.1 M.

X_{Hp}	W_0	d_{App} [nm]
0.20	10	4.6 ± 0.5
0.20	12	5.4 ± 0.5
0.20	15	5.5 ± 0.5
0.20	17	5.9 ± 0.5
0.37	5	4.1 ± 0.5
0.37	10	5.0 ± 0.5
0.37	12	5.8 ± 0.5
0.37	15	5.9 ± 0.5
0.37	17	6.1 ± 0.5
0.58	15	7.2 ± 0.5
0.58	20	9.8 ± 0.5
0.58	25	11.0 ± 0.5

The linear tendency observed in Figure 1 shows that water is effectively sequestrated by AOT to yield RMs in every solvent blend studied, and the RMs consist of discrete spherical droplets. Moreover, we also found that the droplet size of the RMs increases significantly as the *n*-heptane content increases in the nonpolar phase at any W_0 value studied, as was previously observed,[14] even very close to the phase boundary collapse. In that work, it was suggested that as the toluene concentration increases, the droplet–droplet attractive interactions (Scheme 2) are "switched off". As the kinetic effect of the droplet collisions (continually occurring as fusion-splitting of droplets in RM equilibrium) occurs over a millisecond–microsecond timescale for *n*-heptane/AOT RMs, the addition of a "bad" solvent makes the aggregation of droplets an extremely rapid process, followed by a much slower gravitational settling, and this results in an eventual phase resolution of the coarse emulsion droplets.[14,43] On the contrary, by increasing the toluene concentration ("good" solvent) at a fixed temperature within the stability region of the phase diagram, the attractive interactions between particles decrease with the consequent decrease of the RM droplet sizes.[14] Herein, from a thermodynamic point of view, it may be considered

that the addition of *n*-heptane, even far from the phase transition separation, produces larger and more stable AOT RM droplets because interdroplet interactions are favored.

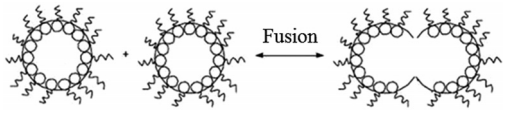

Scheme 2. Schematic representation of interdroplet interactions between two RMs.

There is a direct relationship between the magnitude of interdroplet attractive interactions and the difference between the composition of the interface and the continuous nonpolar phase.[19,21,44] As it is difficult for larger solvent molecules to penetrate the interface, the differences would increase and so would the magnitude of the droplet–droplet interactions. Also, the larger radius of gyration of the longer chains prevents them from close packing on the surfactant interface. The surfactants are optimally packed and, hence, have a larger network attraction. On the other hand, as the oil chain length decreases, the difference between the oil and the surfactant packing decreases, and the net attraction of two droplets is reduced.[45] Following this reasoning, the size increases shown in Figure 1 and Table 2 can be explained by considering the changes in the AOT interfacial composition as the *n*-heptane content increases. In this sense, we note that oil penetration to the interface is thought to be a major factor that affects the interactions, although the origin of attractive forces in RMs is still not clear; it seems that the oil penetration to the interface plays a major role in the droplet–droplet interactions. The greater the oil penetration, the smaller the difference in composition between the interface and the nonpolar phase, and the weaker interdroplet interactions give larger and thermodynamically more stable AOT RMs. Thus, the rigid benzene molecules (V_M = 89.8 $cm^3 mol^{-1}$) can penetrate more easily into the AOT RM interface in comparison with *n*-heptane (V_M = 146.5 $cm^3 mol^{-1}$); consequently, benzene/AOT RMs have smaller droplet sizes than *n*-heptane/AOT RMs at the same W_0 value.[10,26,46,47]

The RM droplet sizes depend, among many other variables, on the effective packing parameter of the surfactants, v/al_c, in which v and l_c are the volume and the length of the hydrocarbon chain, respectively, and a is the surfactant head group area.[48] RM sizes are larger when the surfactant packing parameter values are smaller.[49,50] The DLS results show that as the *n*-heptane mole fraction increases in AOT RMs, the interdroplet interaction also increases, and as a result the RM droplet sizes increase. Therefore, as the *n*-heptane content increases, the overlap between droplets probably causes the removal of benzene molecules from the interface.[19] Under these conditions, the v and the surfactant packing parameter values decrease, and the droplet sizes increase. Also, the water–AOT interactions increase the a value of the surfactant; consequently, the surfactant packing parameter decreases, and the RM droplet size increases.[48,51]

In summary, water–surfactant interactions increase the effective interfacial area by decreasing the surfactant packing parameter and increasing the RM size. In this way, as the *n*-heptane content increases, the water–AOT interactions would be favored and the effective interfacial area value would become larger with a consequent decrease in the surfactant packing parameter. As a result, two main effects can be invoked to understand how RMs droplet sizes change: (1) the magnitude of the interdroplet interaction owing to the kind of external solvent and (2) the interaction between water and the RM interface. Both phenomena are possible explanations for the growth of the size of RM droplets as the *n*-heptane content increases.

Having shown the tremendous impact of the solvent blend composition on the droplet–droplet interactions (Scheme 2), we considered it necessary to go a step further and apply the above results in the design of RMs with specific nanoreactor characteristics. It has long been known that RMs can be used as nanotemplates for nanoparticle synthesis. In the literature it is possible to find quite an amount of work in which the synthesis in RMs is typically controlled by changing the W_0 value, the concentration of the precursors, the presence of additives, the cosurfactant, and/or the RM concentration.[32–34] Surprisingly, there are very few reports on the effect of the change in the external solvent composition on the nanoparticle size for RM nanoreactors. Salabat et al.[14] investigated the solvent composition by using silica nanoparticles stabilized by AOT; however, those nanoparticles were not synthesized by mixing two different RMs. Also, the aggregation and stability of model AOT-stabilized silica nanoparticles in different solvents were investigated to further explore these solvent effects. For stabilization of silica nanoparticles, more compact solvent molecules such as toluene are better than longer chain molecules such as dodecane. On the other hand, Bagwe et al.[52] have studied the effect that cyclohexane, *n*-heptane, and decane/AOT RMs have on silver chloride nanoparticles. Unfortunately, the work does not provide clear evidence about the nanoparticle size and the interdroplet interactions. For example, the authors suggest that the interdroplet interactions are stronger and the sizes of the silver chloride nanoparticles obtained are smaller when decane is used as the external solvent.

Thus, it is evident that the mechanism for RMs to act as nanotemplates is not well understood. To get deeper into this complex question and on the basis of the hypothesis that droplet–droplet interactions are one of the key factors for nanoparticle growth, we will show in the next section results on gold nanoparticle synthesis with two different AOT RMs in which the droplet–droplet interactions are very different. Specifically, we will keep all the variables such as surfactant concentration, temperature, and W_0 values constant and only change the external solvent composition. With these types of experiments, we can use a known nanoparticle synthesis to learn more about how the RM interactions alone affect the nanoparticle sizes.

AOT RMs as Nanoreactors

Considering the results obtained for the different droplet–droplet interactions upon changing the solvent blend composition, we decided to evaluate the AOT RMs as nanoreactors for nanoparticle synthesis in extreme solvent blend conditions (100% *n*-heptane and 100% benzene) by using the methodology described above. Accordingly, it is expected that the channel formed during the fusion process of two droplets in which the material in the RMs is exchanged would be favored for RMs with greater droplet–droplet interactions, that is, they will be favored with *n*-heptane as the organic phase and disfavored with benzene.

Figure 2a shows the absorption spectrum of gold nanoparticles (NPs) synthesized in *n*-heptane/AOT/water RMs at W_0 = 6. The absorption maximum of the surface plasmon resonance (SPR) of the synthesized NPs is located at λ_{max} = 516 nm. The large width and the small intensity of the SPR peak indicates the small size of the formed particles. Figure 2 (b) shows a TEM picture of the NPs and confirms the formation of small, spherical, and highly monodispersed gold NPs with a size of 8 ± 1 nm, as can be seen in the size distribution plot (Figure 2, c); this is similar to the droplet size of the aqueous RMs. It is important to note that the NPs do not interact with each other, and this demonstrates the excellent role of AOT as a stabilizing agent. The high monodispersity of the NPs indicates a fast nucleation process. As the initial concentration of Au ions per droplet (0.6 M) is very small, the results indicate that a fast interchange of reactants should occur during the nucleation process. These results agree with the fact that the droplet–droplet interactions are favored and the rate of material exchange among micelles is increased in these RMs (with *n*-heptane as nonpolar solvent). Thus, the unique AOT interfacial composition favors the interchange of precursors, and the reduction process occurs, leading to a fast nucleation process. As a result, stable gold NPs can be synthesized, and the AOT acts not only acts as part of the nanoreactor but also as the stabilizing agent.

The situation is completely different when the gold nanoparticle synthesis is performed in RMs formed from benzene/AOT/water, in which the droplet–droplet interactions are disfavored. In these RMs, the results (Figure S1a) indicate that the gold particles do not show the characteristic SPR absorption band of gold NPs. Instead, they only show a decreasing absorption in the UV region with a main shoulder at ca. 270 nm.

Figure S1b displays a TEM micrograph of the sample, which shows only the presence of particles smaller than 1 nm; these sizes are below the equipment resolution and suggest that subnanometer atom clusters have formed. Here, the system has an intense fluorescence emission, characteristic of atom clusters (we checked that the fluorescence emission did not occur in the corresponding precursors). Figure 3 shows the fluorescence emission spectra of the clusters formed in these RMs, excited at different wavelengths.

The emission spectrum shows the highest intensity when excited at λ_{exc} = 290 nm and has an emission maximum at

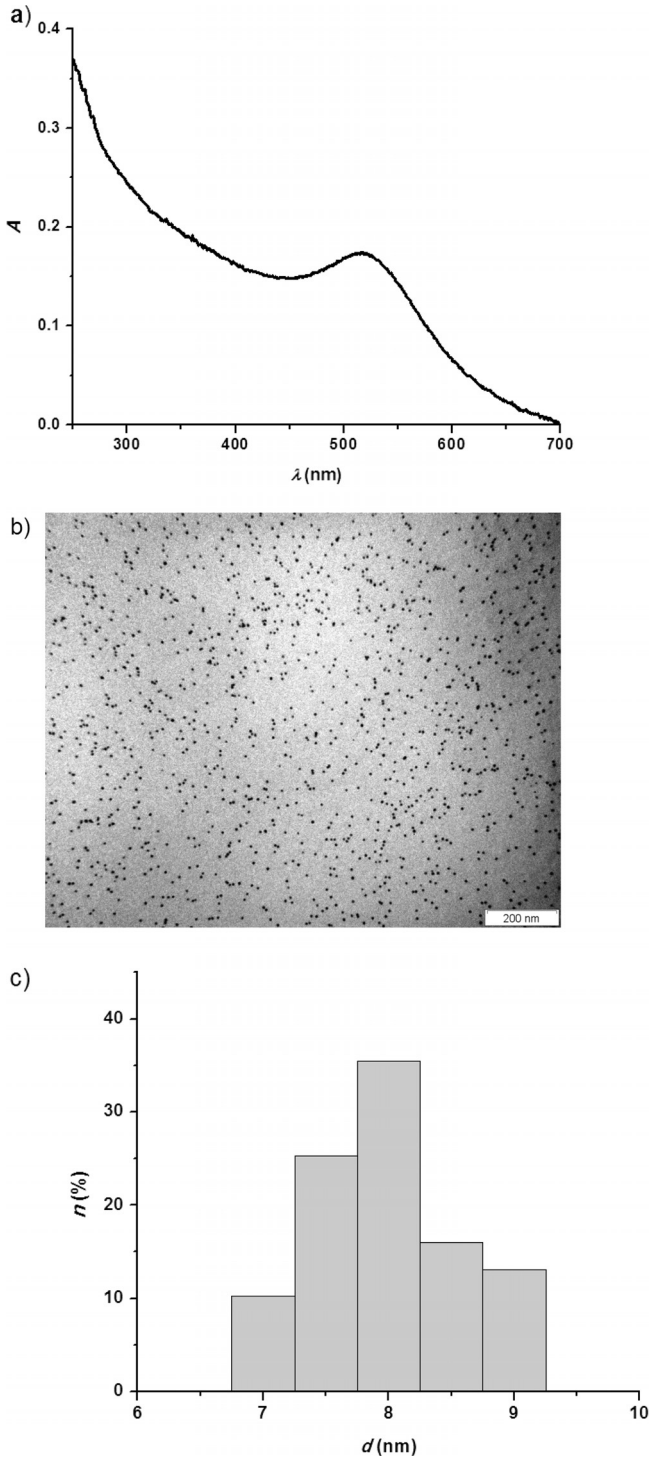

Figure 2. (a) Absorption spectrum and (b) TEM micrographs of gold nanoparticles synthesized in *n*-heptane/AOT/water RMs. (c) Histogram by number (*n*) of the gold nanoparticles distribution. [AOT] = 0.1 M, W_0 = 6. An empty AOT RM solution was used as a blank in (a).

λ_{emi} = 345 nm. Interestingly, when the excitation wavelength is changed, the wavelength emission band is the same; this indicates the formation of a relatively monodispersed cluster sample. By applying just the simple Jellium model ($E_g = E_F/N^{1/3}$, where E_g is the cluster band gap, E_F is the Fermi

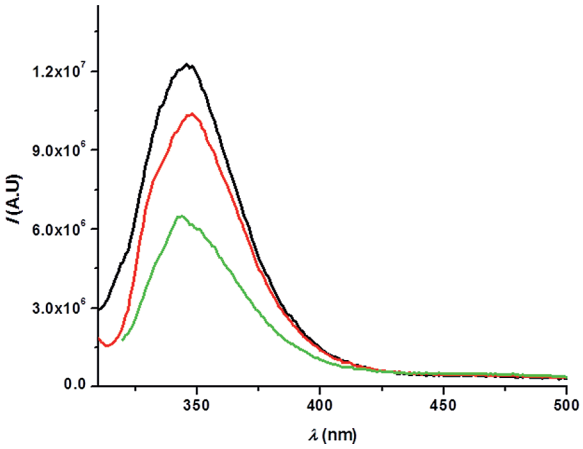

Figure 3. Emission spectra of the subnanometer particles synthesized in benzene/AOT/$HAuCl_4$/N_2H_4 RMs at λ_{exc} = 290 (black), 300 (red), and 310 nm (green). [AOT] = 0.1 M, W_0 = 6.

level, which is 5.3 eV for gold, and N is the number of atoms in the cluster), the emission would correspond to the formation of a Au_N cluster with $N \approx 3$. These results agree with those for Au_2–Au_3 clusters obtained before by electrochemical techniques.[53] More experiments are necessary to determine the specific size, structure, and properties of the subnanometric gold clusters obtained in benzene/AOT RMs. These experiments are underway in our laboratory and are outside the scope of this study; however, the high monodispersity of the clusters produced by this simple method can be noted, as it can be deduced by the presence of only one photoluminescence emission peak. Interestingly, the formation of clusters instead of NPs occurs when RMs with very small droplet sizes (ca. 3.2 nm) are used and there is poor material exchange among the micelles owing to unfavorable droplet–droplet interactions. This confirms previous results that showed that clusters are preferably formed by a kinetically controlled process given by low reaction rates, such as those provided by microemulsion techniques.[54] The important point here is that we obtained gold clusters much smaller than the RMs and the common nanoparticle sizes obtained in RMs by using benzene/AOT RMs to tune only the interdroplet interactions. These interactions were obtained by changing the external solvent, which provides a simple way to produce subnanometer clusters by the microemulsion technique. As these tiny clusters are very active in catalytic applications,[37] including the formation of anisotropic nanostructures[38] and photocatalysis,[38] this simple synthetic method could be of large importance in many applications.

The results of this work show the importance of understanding the behavior of RMs to apply them in a specific field. We have developed an interesting way to use these organized systems for a controlled methodology to generate nanoparticles or clusters just by changes to the RM composition; this could be very useful for the preparation of nanocomposites for many applications.

Studies with C343 as a Molecular Probe

As there are no reports of the direct monitoring of these effects (interdroplet and water–surfactant interactions) on the AOT interface properties, and as C343 inter/intramolecular hydrogen-bond interactions depend dramatically on the polarity of the medium,[55] we used the spectroscopy of C343 to gain more insights. Previous results are discussed in the Supporting Information. In summary, the use of C343, which is an interesting molecule as its spectroscopy is sensitive not only to polarity and hydrogen-bond interactions but also to inter/intramolecular hydrogen-bond competition, shows that when benzene dominates the AOT interface composition, water molecules penetrate to the oil side of the interface, the micropolarity increases, and the C343 intramolecular hydrogen-bonds diminish. On the contrary, when *n*-heptane dominates the RM interfacial composition, the micropolarity decreases, there is no water penetration to the oil side of the interface as water molecules are strongly involved in hydrogen-bond interactions with the AOT sulfonate groups, and the C343 intramolecular hydrogen-bond interactions are favored.

Conclusions

We have investigated the effect of the solvent blend on the interfacial properties of the anionic AOT reverse micellar media. By using the DLS technique and the spectroscopy of C343, we showed that the AOT droplet sizes, the interfacial micropolarity, and the water–AOT interactions depend dramatically on the composition of the nonpolar organic medium. The results indicate that not only does the size of the AOT RMs change upon the addition of *n*-heptane but the interfacial composition of the AOT RMs also varies with the nonpolar phase blend. Also, the spectroscopic behavior of C343 was carefully monitored in every AOT RM system, and the surfactant concentration was changed to obtain the right conditions for the dye to be present at the RM interface as a monomer.

The DLS experiments show that the RM droplet sizes are larger as X_{Hp} increases, and the benzene molecules are expelled from the interface. To understand the properties of the RM interface, it is crucial to use them as a nanoreactor. As particle size control strongly depends on droplet–droplet interactions and interfacial composition, we could anticipate a dramatic effect on the nanoparticle sizes and polydispersity as the composition of the organic solvent blend changes. The results show that AOT RMs formed in *n*-heptane create small, monodisperse, and highly concentrated gold nanoparticles, whereas AOT RMs prepared in benzene seem to create subnanometer gold clusters. In this way, our results offer a new appealing way to focus the production of nanoparticles into subnanometer clusters, which are one of the hottest current topics in nanoparticle synthesis. We hope that these results will contribute to advances in the field of nanoparticle synthesis and separation processes, topics that we are investigating in our laboratory.

Experimental Section

Materials

Benzene and *n*-heptane (Hp) were purchased from Merck (both HPLC grade) and used without further purification. Coumarin 343 (C343, Exciton) was used as received.

Sodium 1,4-bis(2-ethylhexyl) sulfosuccinate (AOT, Sigma, >99% purity) was used as received and kept under vacuum over P_2O_5 to minimize water absorption. The absorption bands of 1-methyl-8-oxyquinolinium betaine were used to check the absence of acidic impurities.[10] Ultrapure water was obtained from a Labconco 90901-01 purification system. For the synthesis of gold nanoparticles, tetrachloroauric acid ($HAuCl_4$, Sigma–Aldrich) as precursor and hydrazine (N_2H_4, Sigma–Aldrich) as reducing agent were used as received.

Methods

The *n*-heptane:benzene blends at any *n*-heptane bulk mole fraction (X_{Hp}) were prepared by weight. The stock solutions of AOT RMs in *n*-heptane:benzene mixtures were prepared by mass and volumetric dilution. To obtain optically clear solutions, they were shaken in a sonication bath, and water was added by using a calibrated microsyringe. The amount of water present in the system is expressed as the molar ratio between the polar solvent and the surfactant, $W_0 = [H_2O]/[AOT]$. The lowest value for W_0 ($W_0 = 0$) corresponds to a system without the addition of water.

To introduce C343 into the RM solutions, a 0.01 M solution was prepared in acetonitrile (Sintorgan HPLC quality). The appropriate amount of this solution to obtain a given concentration (6.0×10^{-6} M) of the probe in the RMs was transferred into a volumetric flask, and the acetonitrile was evaporated by bubbling dry N_2; then, the RM solution was added to the residue to obtain [AOT] = 0.30 M. The stock 0.30 M solution of AOT and C343 was agitated in a sonication bath until the RM solution was optically clear. To the cell containing C343 (2 mL) of the same concentration in the different *n*-heptane:benzene blends, we added the appropriate amount of surfactant and molecular probe stock solution to obtain a given concentration of surfactant in the micellar media. In this way, the absorption and emission of the molecular probe was not affected by dilution. All experimental points were measured three times with different prepared samples. The pooled standard deviation was less than 5%. In all the cases, the temperature was kept at 25 ± 0.2 °C.

Gold nanoparticles were synthesized in RMs by using the methodology described by Lopez-Quintela.[32] A solution of AOT RMs in benzene or *n*-heptane containing tetrachloroauric acid dissolved at [AOT] = 0.1 M and $W_0 = 6$ and another containing hydrazine dissolved in RMs with the same AOT concentration and $W_0 = 6$ were prepared. The reduction process occurs when the two AOT RMs systems are mixed by magnetic agitation at room temperature. The concentration of the metal ions and reducing agent (calculated from the volume of aqueous solution) were kept constant at a $HAuCl_4$:N_2H_4 molar ratio of 1:6.

General

UV/Vis spectra were recorded by using a Shimadzu 2401 spectrophotometer with a thermostatted sample holder. A Spex Fluoromax apparatus was employed for the fluorescent measurements. Corrected fluorescence spectra were obtained by using the correction file provided by the manufacturer.

All of the DLS experiments were performed at a fixed AOT concentration of 0.1 M. Hence, the RM solutions were not at infinite dilution, and we considered it appropriate to introduce an apparent hydrodynamic diameter (d_{App}) to enable comparison with our system as it was used before.[14,22] The apparent hydrodynamic diameters of the different AOT RMs were determined by dynamic light scattering (DLS, Malvern 4700 with goniometer) with an argon-ion laser operating at 488 nm. AOT RM samples were filtered by using an Acrodisc with a 0.2 μm polytetrafluoroethylene (PTFE) membrane (Sigma). For the DLS analyses, the viscosities and refractive indices of the solvent blends are required; the viscosities of *n*-heptane:benzene systems were taken from the literature.[56] The refractive indices of the solvent mixtures were calculated by using thr first-order approximation shown in Equation (1), ηD1 and ηD2 are the pure solvent refractive indices.

$$\eta D = X1\eta D1 + X2\eta D2 \quad (1)$$

The effect of temperature on ηD of these solvents was small enough to be ignored. This approximation gives good and reliable results.

Thirty independent size measurements were made for each individual sample at the scattering angle of 90°; the polydispersity indexes of the experiments were always below 0.2. The algorithm used was CONTIN. The apparent hydrodynamic diameter values reported were weighted by intensity, volume, and/or number as no differences were observed. The DLS experiments show that the polydispersity of the AOT RM size is less than 5%. In our experimental conditions, we obtained a resolution of 0.5 nm.

The micrographs were recorded by using a PHILIPS CM-12 microscope at 20–120 kV with a Megaview-II Docu camera and SIS NT Docu software. For TEM studies, the RM samples were placed onto a Formvar-covered copper grid and evaporated slowly.

Supporting Information (see footnote on the first page of this article): Absorption spectra of benzene/AOT/$HAuCl_4$/N_2H_4 RMs, TEM micrographs of the particles synthesized in benzene/AOT/$HAuCl_4$/N_2H_4 RMs, calculation procedure of the partition constants of the molecular probes, critical micellar concentration (cmc) and partition constant (K_p) values for *n*-heptane:benzene/AOT/water RMs, absorption and emission spectra of C343 in *n*-heptane:benzene/AOT RMs.

Acknowledgments

This work was supported by the Consejo Nacional de Investigaciones Científicas y Técnicas (CONICET), Agencia Córdoba Ciencia, Agencia Nacional de Promoción Científica y Técnica, Secretaría de Ciencia y Técnica de la Universidad Nacional de Río Cuarto, Spanish Ministerio de Educación y Ciencia (MEC) (MAT2012-36754-C02-01), and the Spanish Obra Social Fundación La Caixa (2012-CL097). N. M. C., J. J. S., and R. D. F. hold research positions at CONICET. J. A. G thanks CONICET for a research fellowship and Fundacion Carolina for a research fellowship that allows him to travel to the laboratory of M. A. L.-Q.

[1] S. P. Moulik, B. K. Paul, *Adv. Colloid Interface Sci.* **1998**, *78*, 99–195.
[2] V. Uskokovic, M. Drofenik, *Adv. Colloid Interface Sci.* **2007**, *133*, 23–34.
[3] J. J. Silber, M. A. Biasutti, E. Abuin, E. Lissi, *Adv. Colloid Interface Sci.* **1999**, *82*, 189–252.
[4] T. K. De, A. Maitra, *Adv. Colloid Interface Sci.* **1995**, *59*, 95–193.
[5] J. Gu, Z. A. Schelly, *Langmuir* **1997**, *13*, 4256–4266.
[6] D. Mandal, A. Datta, P. S. Kumar, K. Bhattacharyya, *J. Phys. Chem. B* **1998**, *102*, 9070–9073.

[7] R. McNeil, J. K. Thomas, *J. Colloid Interface Sci.* **1981**, *83*, 57–65.
[8] A. Jada, J. Lang, R. Zana, *J. Phys. Chem.* **1990**, *94*, 381–387.
[9] A. Jada, J. Lang, R. Zana, R. Makhloufi, E. Hirsch, S. J. Candau, *J. Phys. Chem.* **1990**, *94*, 387–395.
[10] N. M. Correa, M. A. Biasutti, J. J. Silber, *J. Colloid Interface Sci.* **1995**, *172*, 71–76.
[11] N. M. Correa, N. E. Levinger, *J. Phys. Chem. B* **2006**, *110*, 13050–13061.
[12] D. Grand, A. Dokutchaev, *J. Phys. Chem. B* **1997**, *101*, 3181–3186.
[13] M. D'Angelo, D. Fioretto, G. Onori, A. Santucci, *J. Mol. Struct.* **1996**, *383*, 157–163.
[14] A. Salabat, J. Eastoe, K. J. Mutch, R. F. Tabor, *J. Colloid Interface Sci.* **2008**, *318*, 244–251.
[15] O. Myakonkaya, J. Eastoe, K. J. Mutch, S. Rogers, R. Heenan, I. Grillo, *Langmuir* **2009**, *25*, 2743–2748.
[16] M. J. Hollamby, R. Tabo, K. J. Mutch, K. Trickett, J. Eastoe, R. Heenan, I. Grillo, *Langmuir* **2008**, *24*, 12235–12240.
[17] M. J. Hou, M. Kim, D. O. Shah, *J. Colloid Interface Sci.* **1988**, *123*, 398–412.
[18] A. M. Cazabat, D. Langevin, *J. Chem. Phys.* **1981**, *74*, 3148–3158.
[19] B. Lemaire, P. Bothorel, D. Roux, *J. Phys. Chem.* **1983**, *87*, 1023–1028.
[20] J. S. Huang, *J. Chem. Phys.* **1985**, *82*, 480–484.
[21] A. A. Calje, W. G. M. Agterof, A. Vrij, in: *Micellization, Solubilization and Microemulsions*, vol. 2 (Ed.: K. L. Mittal), Plenum, New York, **1977**, p. 779–790.
[22] F. M. Agazzi, R. D. Falcone, J. J. Silber, N. M. Correa, *J. Phys. Chem. B* **2011**, *115*, 12076–12084.
[23] F. M. Agazzi, J. Rodriguez, R. D. Falcone, J. J. Silber, N. M. Correa, *Langmuir* **2013**, *29*, 3556–3566.
[24] F. Moyano, R. D. Falcone, J. C. Mejuto, J. J. Silber, N. M. Correa, *Chem. Eur. J.* **2010**, *16*, 8887–8893.
[25] D. Blach, N. M. Correa, J. J. Silber, R. D. Falcone, *J. Colloid Interface Sci.* **2011**, *355*, 124–130.
[26] L. García Rio, A. Godoy, P. Rodríguez-Dafonte, *Eur. J. Org. Chem.* **2006**, 3364–3371.
[27] P. R. Majhi, S. P. Moulik, *J. Phys. Chem. B* **1999**, *103*, 5977–5983.
[28] M. Ueda, Z. A. Schelly, *J. Colloid Interface Sci.* **1988**, *124*, 673–676.
[29] K. Mukerjee, S. P. Moulik, D. P. Mukherjee, *Langmuir* **1993**, *9*, 1727–1730.
[30] F. A. Heatley, *J. Chem. Soc. Faraday Trans. 1* **1988**, *84*, 343–354.
[31] S. K. Hait, A. Sanyal, S. P. Moulik, *J. Phys. Chem. B* **2002**, *106*, 12642–12650.
[32] M. A. López-Quintela, *Curr. Opin. Colloid Interface Sci.* **2003**, *8*, 137–144.
[33] A. B. Smetana, J. S. Wang, J. Boeckl, G. J. Brown, C. M. Wai, *Langmuir* **2007**, *23*, 10429–10432.
[34] M. A. Lopez-Quintela, C. Tojo, M. C. Blanco, L. García Río, J. R. Leis, *Curr. Opin. Colloid Interface Sci.* **2004**, *9*, 264–278.
[35] R. Bhattacharya, P. Mukherjee, *Adv. Drug Delivery Rev.* **2008**, *60*, 1289–1306.
[36] P. K. Jain, X. Huang, I. H. El-Sayed, M. A. El-Sayed, *Acc. Chem. Res.* **2008**, *41*, 1578–1586.
[37] A. Corma, P. Concepción, M. Boronat, M. J. Sabater, J. Navas, M. J. Yacaman, E. Larios, A. Posadas, M. A. López-Quintela, D. Buceta, E. Mendoza, G. Guilera, A. Mayoral, *Nat. Chem.* **2013**, *5*, 775–781.
[38] Y. Attia, D. Buceta, C. Blanco-Varela, M. B. Mohamed, G. Barone, M. A. Lopez-Quintela, *J. Am. Chem. Soc.* **2014**, *136*, 1182–1185.
[39] P. D. I. Fletcher, M. F. Galal, B. H. Robinson, *J. Chem. Soc. Faraday Trans. 1* **1984**, *80*, 3307–3314.
[40] E. R. Riter, J. R. Kimmel, E. P. Undiks, N. E. Levinger, *J. Phys. Chem. B* **1997**, *101*, 8292–8297.
[41] J. Eastoe, S. Gold, S. E. Rogers, A. Paul, T. Welton, R. K. Heenan, I. Grillo, *J. Am. Chem. Soc.* **2005**, *127*, 7302–7303.
[42] Y. Gao, N. Li, L. Zheng, X. Bai, L. Yu, X. Zhao, J. Zhang, M. Zhao, Z. Li, *J. Phys. Chem. B* **2007**, *111*, 2506–2513.
[43] P. D. L. Fletcher, A. M. Howe, B. H. Robinson, *J. Chem. Soc. Faraday Trans. 1* **1987**, *83*, 985–1006.
[44] S. Brunetti, D. Roux, A. M. Bellocq, G. Fourche, P. Bothorel, *J. Phys. Chem.* **1983**, *87*, 1028–1034.
[45] J. S. Huang, S. A. Safran, M. W. Kim, G. S. Grest, M. Kotlarchyk, N. Quirke, *Phys. Rev. Lett.* **1984**, *53*, 592–595.
[46] J. Eastoe, K. J. Hetherington, D. Sharpe, D. C. Steytler, S. Egelhaaf, R. K. Heenan, *Langmuir* **1997**, *13*, 2490–2493.
[47] J. Eastoe, K. J. Hetherington, D. Sharpe, J. Dong, R. K. Heenan, D. C. Steytler, *Langmuir* **1996**, *12*, 3876–3880.
[48] A. Maitra, *J. Phys. Chem.* **1984**, *88*, 5122–5125.
[49] Q. Li, T. Li, J. Wu, *J. Colloid Interface Sci.* **2001**, *239*, 522–527.
[50] D. F. Evans, B. W. Ninham, *J. Phys. Chem.* **1986**, *90*, 226–234.
[51] R. D. Falcone, J. J. Silber, N. M. Correa, *Phys. Chem. Chem. Phys.* **2009**, *11*, 11096–11100.
[52] E. P. Bagwe, K. C. Khilar, *Langmuir* **1997**, *13*, 6432–6438.
[53] B. S. González, M. J. Rodriguez, C. Blanco, J. Rivas, M. A. López-Quintela, J. M. G. Martinho, *Nano Lett.* **2010**, *10*, 4217–4221.
[54] J. Calvo, J. Rivas, M. A. López-Quintela, *Synthesis of Subnanometric Nanoparticles, Encyclopedia of Nanotechnology* (Ed.: Bhushan Bharat), Springer, Dordrecht, The Netherlands, **2012**.
[55] J. A. Gutierrez, R. D. Falcone, J. J. Silber, N. M. Correa, *J. Phys. Chem. A* **2010**, *114*, 7326–7330.
[56] H. Iloukhani, M. R. Sameti, J. B. Parsa, *J. Chem. Thermodyn.* **2006**, *38*, 975–982.

Received: December 20, 2013
Published Online: March 13, 2014

